

Development of Java™ components  
for a collaborative problem-solving environment for weld process modeling

Menlo Wu

Energy Research Undergraduate Laboratory Fellowship

Florida International University

Oak Ridge National Laboratory

Oak Ridge, TN 37831

August 11, 2000

Prepared in partial fulfillment of the requirements of the Office of Science, DOE ERULF Program under the direction of Suresh Babu, and Stan David in Metals and Ceramics Division at Oak Ridge National Laboratory.

Participant: \_\_\_\_\_  
Menlo Wu

Research Advisor: \_\_\_\_\_  
Suresh Babu

## Table of Contents

Abstract	3
Introduction	4
Methods and Materials	6
Results	7
Discussion and Conclusion	8
Acknowledgements	9
References	10
Figures	11
Tables	19

## Abstract

Development of Java™ components for a collaborative problem-solving environment for weld process modeling. MENLO WUU (Florida International University, Miami, Florida 33166) Stan David and Suresh Babu (Oak Ridge National Laboratory, Oak Ridge, Tennessee 37831).

The recent advances in network computing and software development have provided a way to use distributed high performance computing for scientific and engineering simulations. Problem-solving environment (PSE) is a complete, integrated software environment for solving a computational problem, or class of related problems. Component-based software engineering (CBSE) is used to facilitate the software integration. Java™ is an ideal programming language in which to develop CBSE because of its ease of use and fast development time. This project pertains to the development of Java™ components for weld process modeling. The first component is a dilution model for determining the weld bead composition as a function of weld bead geometry and alloy composition. The second component is the prediction of the ferrite number given the composition of the alloy. The component will be able to take the composition of alloy and calculate the ferrite content. A sub-component of the ferrite number is the graph of the WRC 1992 diagram.

### Research Category: Computer Science

School Attending:	Florida International University
DOE National Laboratory Attended:	Oak Ridge National Laboratory
Mentor's Name:	Suresh Babu, and Stan David
Phone:	(865) 574-4806
E-mail:	<a href="mailto:babuss@ornl.gov">babuss@ornl.gov</a>
Name:	Menlo Wu
Mailing Address:	19620 NE 10 <sup>th</sup> Ave
City/State/ZIP	N. Miami Beach, FL 33179
Phone:	(305) 653-5147
E-mail:	<a href="mailto:mwu01@fiu.edu">mwu01@fiu.edu</a>
DOE Program:	ERULF

## Introduction

Imagine that welder has just finished welding two pieces of metal only to find out that the weld does not meet standards for its use. The welder would then have to repeat the weld and test again. This iterative procedure leads to expensive and time consuming process development and it is more serious for new and advanced metals and alloys. As a result of this iterative process, new emerging materials research is significantly slowed down. With the help of a collaborative problem-solving environment (PSE) for weld process modeling, this limitation can be removed.

A PSE is used to simulate and model behaviors to solve a problem or a class of related problems. By using distributed high performance computing resources, the PSE would be able to simulate the weld process for the welder. The weld process modeling is widely used for joining structural alloys and determining the characteristics and performance of welds in service conditions. However, weld process modeling involves many physical processes. Therefore a predictive model should be able to consider all or crucial physical processes shown in figure 1. This can be achieved by developing separate smaller models that account for heat transfer, thermo-chemical reactions, phase transformations, and such. All the models would be then integrated together to form a problem solving environment. To implement this, Java™ development environment is ideal because of its fast development time, platform independence, and easy integration of the different smaller process models with the help of a common object request broker architecture (CORBA).

In order to understand the two models presented in this paper, a brief background of metallurgy is given. Metallurgy is the study of science and technology of metals, and the relationship between structures and properties of metals. The microstructure relates to the size,

shape, and orientation of the individual crystals in a piece of material. The crystals are sometimes called grains (Thrower, 14). The microstructure in metals are greatly affected by weld thermal cycles and large gradients in weld compositions. The weld process model attempts to relate these welding process parameters, to thermal cycles. In addition with a knowledge of weld compositions one can predict the microstructural gradients. In this project, the first part focuses on discussing compositional changes due to dilution, and second to relate compositional changes to ferrite formation. The ferrite content determines properties such as brittleness, corrosion, and microstructural evolution during heat treatment (Babu et al. 1997). The microstructure changes from body centered cubic (BCC), alpha phase ferrite (  $\alpha$  ) to face centered cubic (FCC), gamma phase austenite (  $\gamma$  ) at around 723° Celsius. The microstructure goes through another change at around 1400° Celsius, from FCC austenite to BCC delta phase ferrite (  $\delta$  ), shown in figure 2a. The BCC and FCC structure is shown in figure 2b.

The first project is a dilution model. Dilution is important because when different base metals are welded by multi-pass technique, the composition of weld bead changes continuously. As more weld beads overlap, the composition of each bead may change.

The second project, ferrite number prediction is for determining microstructure changes in stainless steel welds and metal properties. The ferrite number along with the WRC diagram developed by Schaeffler and DeLong, indicates microstructure according to the regions bounded by the magenta line (Babu et al. 1997). Figure 3 shows the different regions, F=ferrite, M=martensite, A=austenite. In addition, a model that is based on the free energy change between ferrite and austenite is also used to calculate the ferrite number (Babu et al 1997).

## Materials and Methods

The main material used to develop the ferrite number prediction model and the dilution model was a personal computer with a Pentium 233 MHz, and 128 MBs of RAM. The software used in developing the models were the Java™ development kit (JDK) version 1.2, and the software development environment in CodeWarrior . The computer used Windows NT 4 workstation as the operating system. The models created were also tested on a Linux platform (RedHat version 6.2), as well as a Mac platform with Mac OS 9 as the operating system.

In the dilution model, the first method or step was to decide on the control flow of model. The control flow is an ordered number of steps that the user can make to operate the model and how the program interacts with the user. Next was to decide on the fixed bead sizes, and shapes of the base metals to be welded. After initial discussion, it was decided to have four fixed bead sizes, one custom bead, and three different joints for the base metals to be welded. The next step was to implement the user input interfaces, and the custom bead panel where the user can adjust the shape and size of the bead. The final step was to add the code for the calculation, and implementing double buffering to reduce flickering. Figure 4 shows the layout of the final dilution model.

The methods involved in developing the ferrite number prediction model were first to develop the user interface (UI) to receive the input from the user, then draw and display the graphical WRC diagram, and finally draw the location of the ferrite number, and do the calculations. There were some considerations to consider when designing the UI and creating the diagram such as using layout managers, final appearance of the UI, and overall performance.

## Results

The dilution model was tested by comparing the results to an actual weld. The dilution model is shown in figure 4 with instructions on how to use it. The actual weld (figure 5), shows the beads, and the order in which they were welded. The composition of the filler metal and base metals are listed below the figure. Using a scanning electron microscope (SEM), the composition of a region can be measured. The measurement relies on the detection of X-rays produced by electron impingement on the specimen surface. The figure 6 shows the area where the concentration of aluminum in table 1 is obtained. The dilution model simulation of the weld is shown in figure 7a, along with the compositions of the beads figure 7b. Since bead 3 from the simulation corresponds to the area tested with the SEM, its composition is examined. The weight percent of aluminum in bead 3 is 4.22 percent. Comparing it with the data received from the SEM of the area (Table 1) indicates that the dilution model is reasonably accurate.

The ferrite number prediction model is shown in figure 8 with instructions on how to use the model. It was tested by comparing the results with a Feritscope (shown in figure 9). The stainless steel metals (Chromenar 308, shown in figure 10) that was tested for the ferrite content. Since the stainless steel metal compositions are not completely uniform, the average of the readings taken from the Feritscope is used as the actual ferrite number, shown in table 2. The composition of the 308 metal is given in table 3. A range exists for the Chromium and Nickel content and therefore the ferrite model would have a range as well. Table 4 shows the two extremes of the range (2 through 10). Figures 10a and 10b show the screen shots of the results from the ferrite model. The first extreme (WRC ferrite number = 10, Function fit = 9) is similar to the average values (W484=12.4, LT-C=14.5) by the Feritscope in table 2.

## Discussion and Conclusion

The composition of aluminum from the dilution model is not exactly equal to the results of the SEM-EDX because several assumptions are made in the model. The dilution model assumes that complete mixing occurs in the weld bead. This means that the bead compositions and base metal compositions are uniform. Therefore when the bead is overlapped the mixing in the overlapped regions is uniform as well. However, complete mixing often does not occur in actual welds. Another assumption is that the user placed the beads in the same location as in the actual weld. While this is possible, it is highly unlikely. A restriction of the model is that the custom bead shape incorporates only two curves and cannot be rotated therefore may not be the best bead shape used during the simulation. A solution would be to allow the user to draw the bead shape with the mouse or add additional curves to the custom bead shape area. An additional constraint on the model is the limited number of different joints to be welded. The current the model supports only three fixed joints. To improve the model and make it more flexible, options for the user to draw the joints, change the angle of the joint, and distance apart should be added.

The ferrite number prediction model produced results that were similar to the Feritscope, however the range of the ferrite number from the model varied from 2 to 9 using the function fit method. This is due partly from the Feritscope, shape of the weld, and dissimilar composition in some parts of the weld. The Feritscope is not able to accurately measure the ferrite number if the weld curvature of the weld bead is over a certain value, also the Feritscope may produce errors as well. This is why several readings were taken from each of the weld metals with the Feritscope. While the model assumes uniform composition, the weld metals are not completely uniform, and



complete mixing might not have occurred during welding. These possibilities led to error when comparing the readings from the Feritscope and the model. Additional improvements may be to make the model operate in reverse direction. The user would be able to enter a ferrite number, and the model produce the different combination of compositions that satisfy that ferrite number.

An integration of the two models would be the beginning of a problem-solving environment for weld process modeling. The models would then be able to send information to each other via a network and server. This would allow a user to simulate a weld in the dilution model, and determine the ferrite number for each bead. In order to make this possible, the models would have to be able to communicate over a network to access the models needed to do the computation. To implement this, the models which are currently applets should be made into Java Beans to ease transportability, and the use of CORBA or remote method invocation (RMI) to link the models together. In the end, many different models will be implemented and integrated into the weld process model. Anyone with access to the internet will be able to use the weld process model to simulate a weld.

## **Acknowledgements**

I thank the United States Department of Energy -- Office of Science for giving me the opportunity to participate in the Materials Joining and Nondestructive Evaluation Laboratory.

My thanks also go to my mentors Suresh Babu and Stan David, and the entire staff at the Materials Joining and Nondestructive Evaluation Laboratory at Oak Ridge National Laboratory in Oak Ridge, Tennessee.

The research described in this paper was performed at the Materials Joining and Nondestructive Evaluation Laboratory, a national scientific user facility sponsored by the United States Department of Energy and located at Oak Ridge National Laboratory.

## References

Babu, S.S. (September 1991). Acicular Ferrite & Bainite in Fe-Cr-C weld deposits,

University of Cambridge, pp. 16.

Babu, S.S., Vitek, J.M., Iskander, Y.S., David, S.A. (1997). “New model for prediction of ferrite number of stainless steel welds.” Science and Technology of Welding and Joining, Vol.

2 No. 6 , pp. 279-282.

Thrower, Peter A. (1992). Materials in Today's World, revised Ed. McGraw-Hill, Inc.

pp. 14, 46.

## Figures

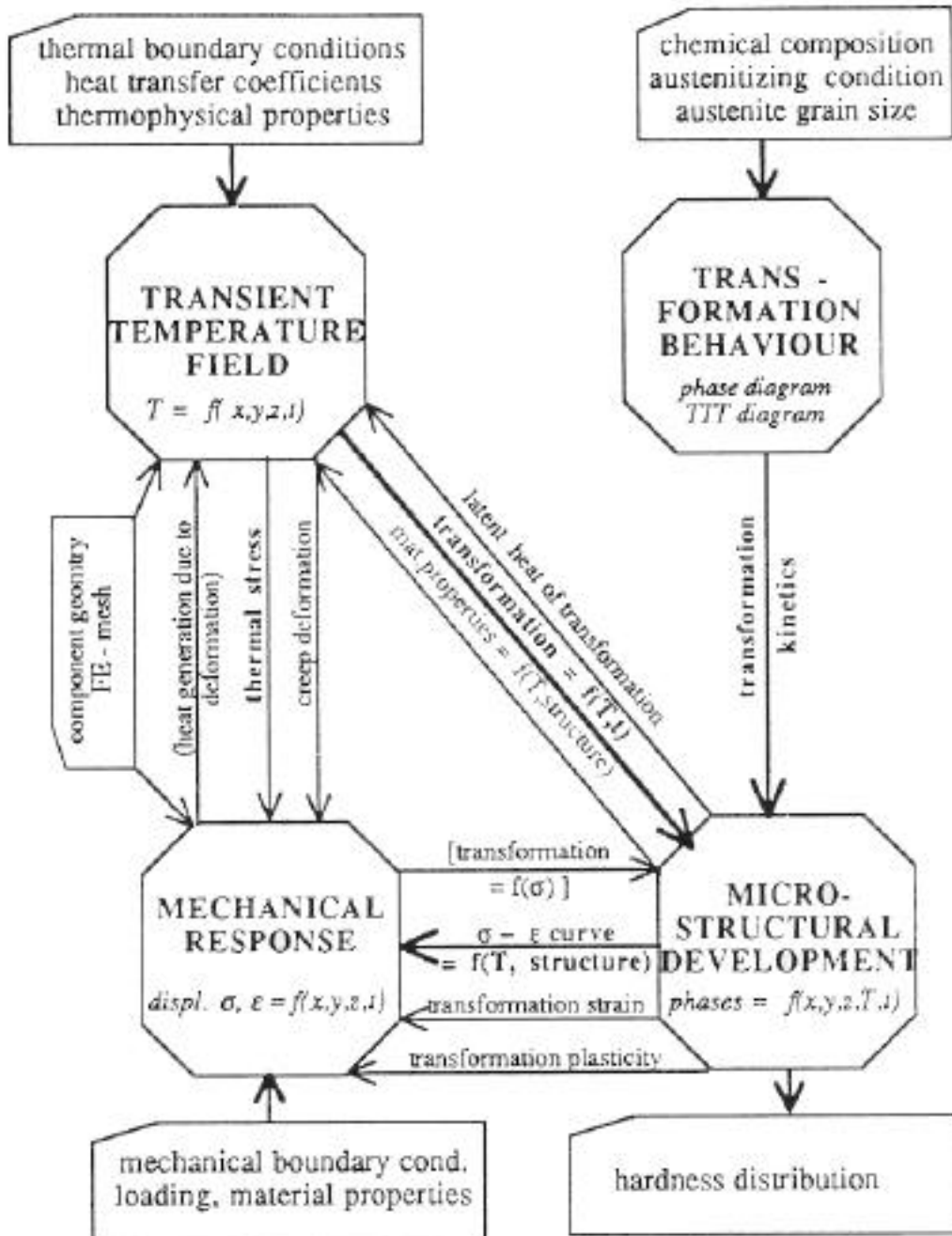


Figure 1. Modeling phase transformations in steels in response to thermochemical conditions. From Babu page 16.

## Figures

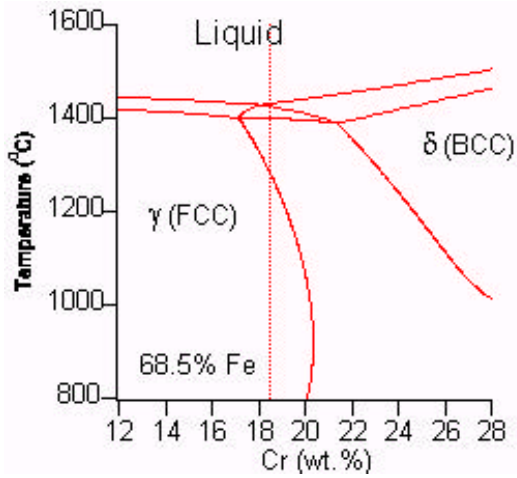


Figure 2a. Phase diagram of gamma FCC, Liquid, and delta BCC

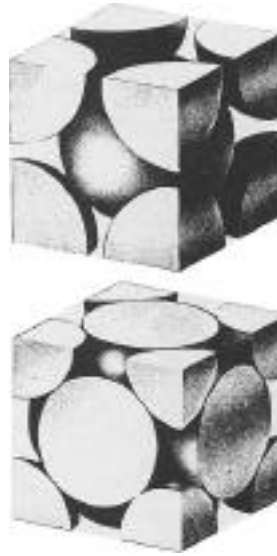


Figure 2b.

Shows BCC structure

Shows FCC structure

From Throver 46.

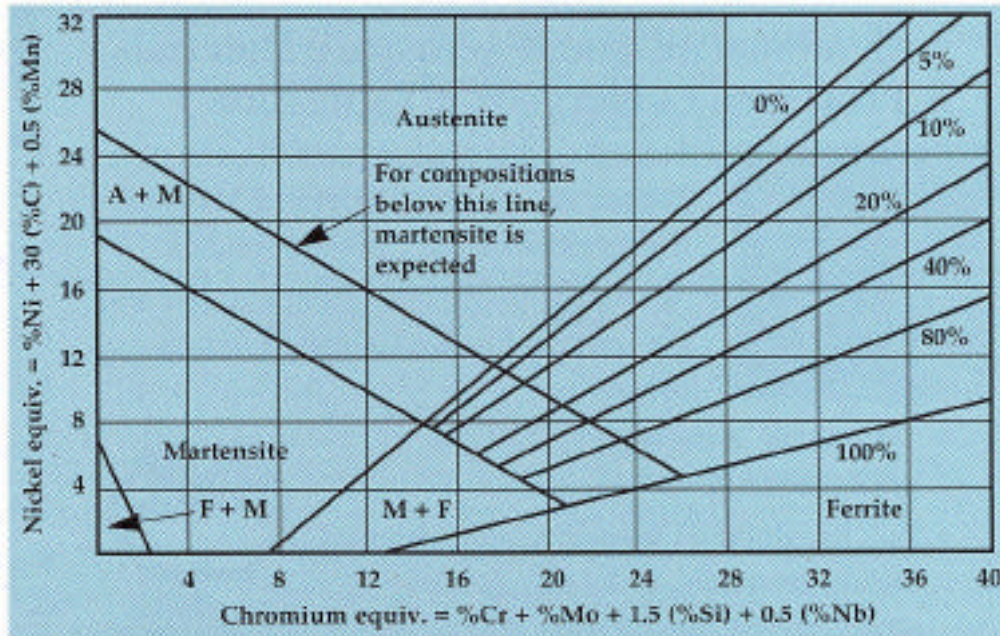


Figure 3. The 1949 Shaeffler Diagram, shows when ferrite, austenite, and martensite are formed.

## Figures

**Instructions:** Follow instructions in applet.

**1** Working area showing Base Metal 1 and Base Metal 2.

**2** Select Metal Joint Type: Angle & Angle (V-type)

**3** Bead Shapes: Remove Bead, Clear All

**4** Custom Bead Shape: Reset Bead

**5** Enter Filler Metal Composition

C wt. %	0.03	Si wt. %	0.49	Mn wt. %	1.52
Mo wt. %	0.15	N wt. %	0.085	Nb wt. %	0.0
P wt. %	0.0	S wt. %	0.0	Ni wt. %	9.7
Al wt. %	0.09	Cr wt. %	18.9	Ti wt. %	0.01

**6** Output Table

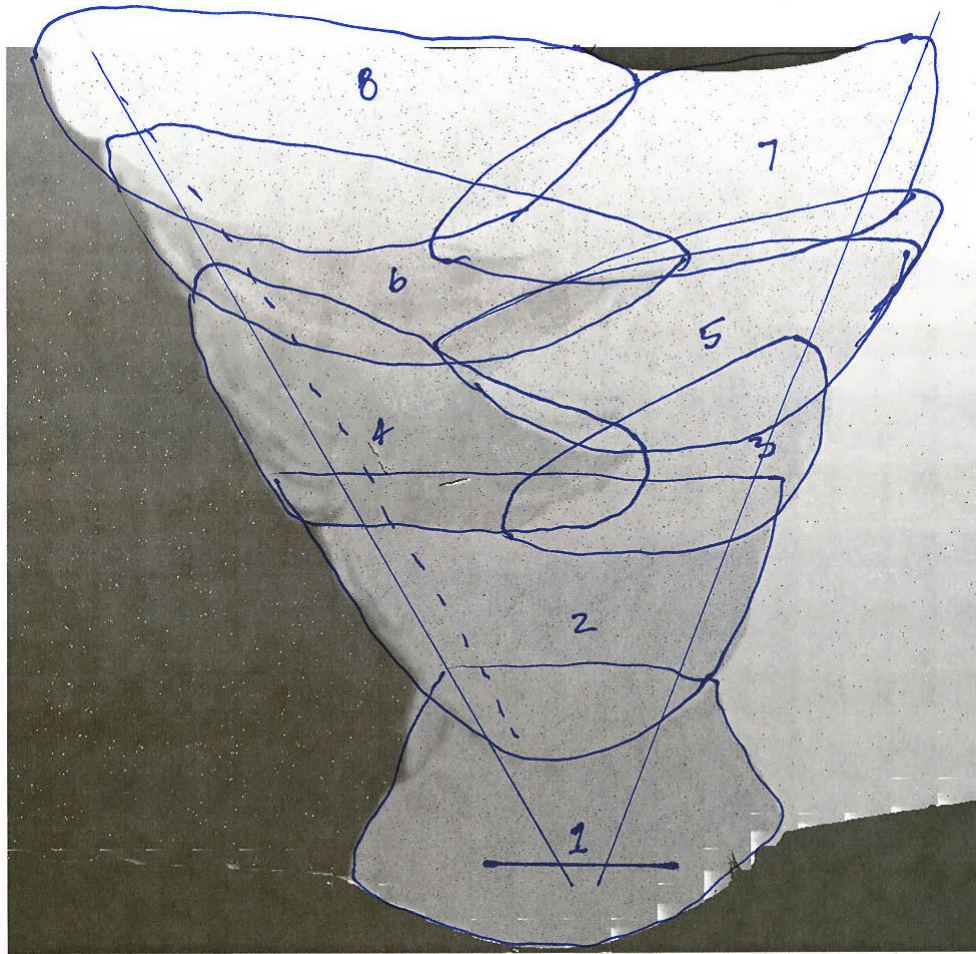
Figure 4. Shows the dilution model graphical user interface.

### Instructions

- 1.) The working area, the weld bead is added here.
- 2.) Selection box to select the metal joint type, three types: Angle & Angle (V shape), Angle & Rectangle, Angle & Angle (Y shape)
- 3.) Fixed bead selection area. Click, and drag the bead to the work area to place bead. Remove bead button removes the last bead. Clear all button clears all beads and compositions including filler metal and base metal compositions.
- 4.) Custom bead area. User can create a custom bead shape and add it to the work area. The red and blue control squares move horizontally only. Green control squares moves horizontally, and vertically till the imaginary line formed by the red and green squares.
- 5.) Dynamic message and control area. The message changes when the Next button is pushed. After filler metal and base metal compositions are entered, the Next button disappears, and a Selection box (used to select a bead) and Compute button (used to compute the bead composition of the selected bead) appears.
- 6.) Outputs in a table format the filler metal, base metals, and beads composition.



## Figures



BS EZ03867A F/Al-Stainless Steel Weld

1mm

### Composition of the weld

Base Metal 1 = Fe - 24 Al

Base Metal 2 (304L) = Fe - 0.03 C - 2 Mn - 1 Si - 19 Cr - 10.5 Ni - 0.045 P - 0.03 S

Filler Metal (308L) = Fe - 0.04 C - 1.5 Mn - 1 Si - 19 Cr - 10 Ni - 0.04 P - 0.02 S - 0.5 Mo - 0.5 Cu

Figure 5. Shows an actual stainless steel weld. Base Metal 1 on left, Base Metal 2 right.

Compositions of the filler metal (FM), base metal 1 (BM1), and base metal 2 (BM2) are listed.

The beads are circled and numbered in the order in which they were welded.

## Figures

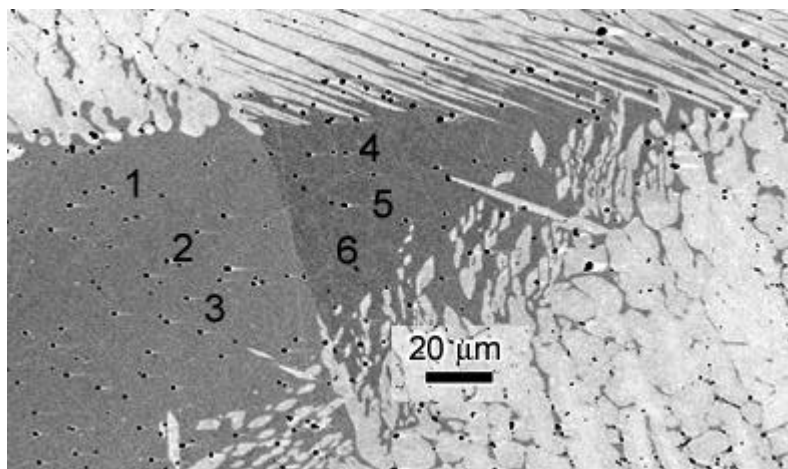
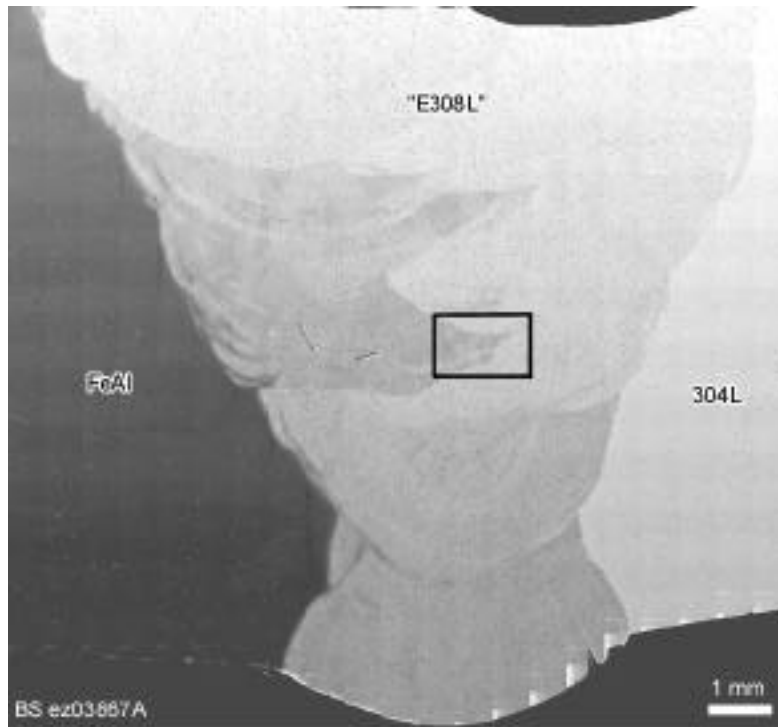


Figure 6. Shows zoomed in area of the original weld, where the six samples were taken.



## Figures

Select Metal Joint Type:

Composition of Bead # 3

C wt. %	<input type="text" value="0.0319"/>	Si wt. %	<input type="text" value="0.82411"/>	Mn wt. %	<input type="text" value="1.2844"/>
Mo wt. %	<input type="text" value="0.3637"/>	N wt. %	<input type="text" value="0.0"/>	Nb wt. %	<input type="text" value="0.0"/>
P wt. %	<input type="text" value="0.0334"/>	S wt. %	<input type="text" value="0.0174"/>	Ni wt. %	<input type="text" value="8.2894"/>
Al wt. %	<input type="text" value="4.2213"/>	Cr wt. %	<input type="text" value="15.6581"/>	Ti wt. %	<input type="text" value="0.0"/>

Select bead then click Compute:

Figure 7a. Shows the simulation of the weld in figure 5.

Elements in (wt %)	C	Mn	Si	Cr	Ni	Mo	N	Nb	Ti	Al	P	S
Filler Metal 1	0.04	1.5	1.0	18.0	10.0	0.5	0.0	0.0	0.0	0.0	0.04	0.02
Base Metal 1	0.0	0.0	0.0	0.0	0.0	0.0	0.0	0.0	0.0	24.0	0.0	0.0
Base Metal 2	0.03	2.0	1.0	18.0	10.5	0.0	0.0	0.0	0.0	0.0	0.045	0.03
Bead 0	0.025	1.209	0.701	13.32	7.168	0.193	0.0	0.0	0.0	7.175	0.03	0.017
Bead 1	0.031	1.328	0.824	15.884	8.338	0.321	0.0	0.0	0.0	4.214	0.034	0.018
Bead 2	0.035	1.553	0.948	18.02	9.615	0.344	0.0	0.0	0.0	1.237	0.039	0.022
Bead 3	0.032	1.294	0.824	16.850	8.289	0.364	0.0	0.0	0.0	4.221	0.033	0.017
Bead 4	0.037	1.528	0.87	18.426	9.760	0.414	0.0	0.0	0.0	0.725	0.04	0.021
Bead 5	0.034	1.323	0.866	16.459	8.686	0.409	0.0	0.0	0.0	3.21	0.035	0.018
Bead 6	0.038	1.522	0.973	18.487	9.793	0.424	0.0	0.0	0.0	0.648	0.04	0.021
Bead 7	0.036	1.387	0.918	17.436	9.187	0.448	0.0	0.0	0.0	1.976	0.037	0.019

Figure 7b. Shows all the compositions of the simulation.

## Figures

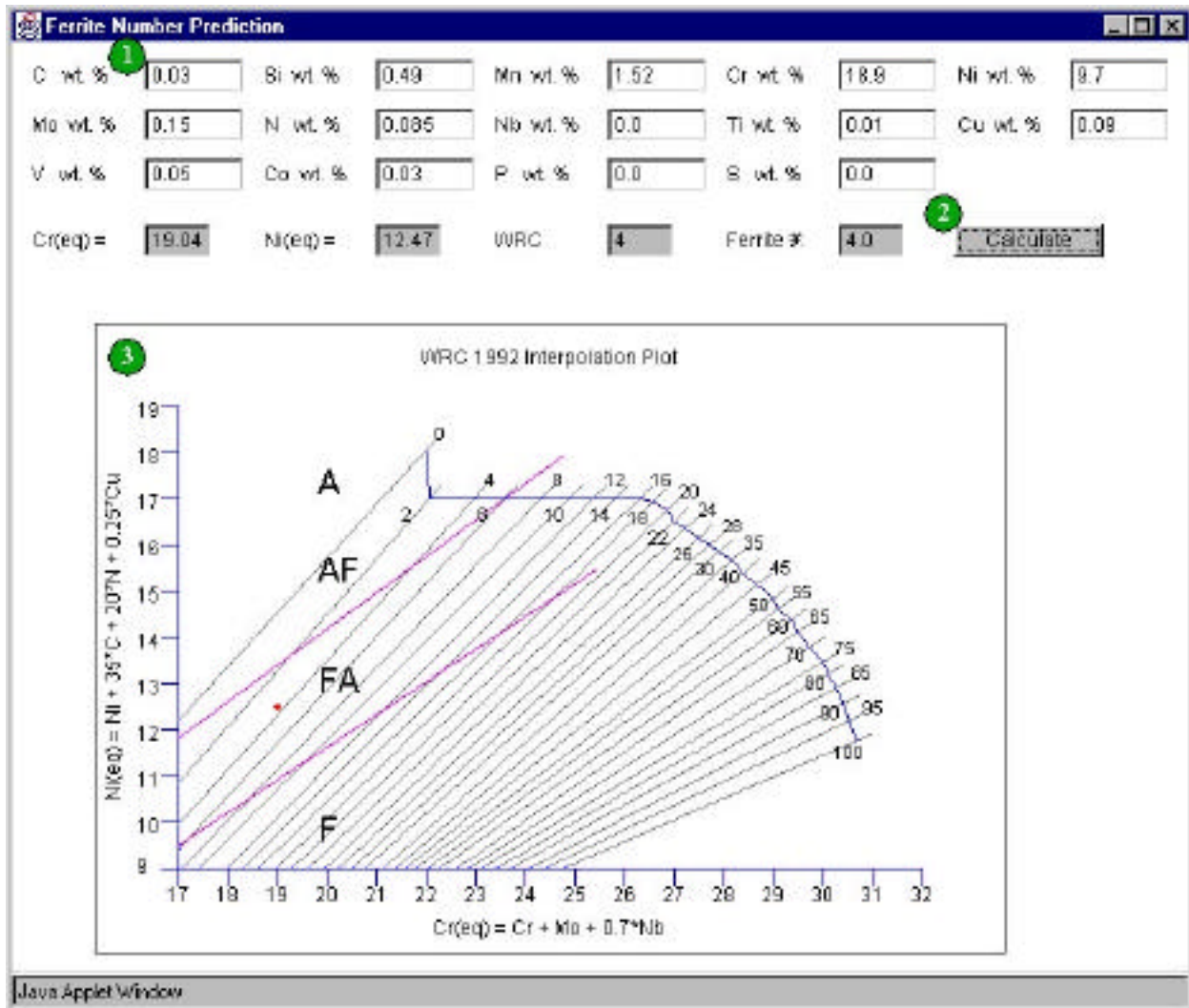


Figure 8. Shows the Ferrite Number Prediction model.

### **Instructions**

- 1.) User enters the composition here.
- 2.) After entering the composition, push calculate, here.
- 3.) Plot of the WRC diagram. The red dot indicates the location of the ferrite number according to the Cr(eq) and Ni(eq). The WRC ferrite number is interpolated from the graph, and the ferrite number is calculated using the function fit method.

\*Note: The WRC ferrite number is results in Not-A-Number (NaN) if the red dot is outside the boundaries of the gray lines and the bounding blue lines.

## Figures



Figure 9.

The Feritscope MP3C is from Fischer used to measure the ferrite content.

The probe is placed on the welded surface to measure the ferrite number.



Figure 10, shows the two weld pieces tested for the ferrite number.

The first piece (W484) dimensions are 0.5" x 2" x 10", and the second (LT-C) is 1" x 3.5" x 4" approximately. Both are 308 stainless steel metals.

## Figures

Figure 11a.

Using Cr = 21 %, and Ni = 10%.  
This shows one extreme,  
WRC=10 and FN=9 for the  
composition of the 308 metals.

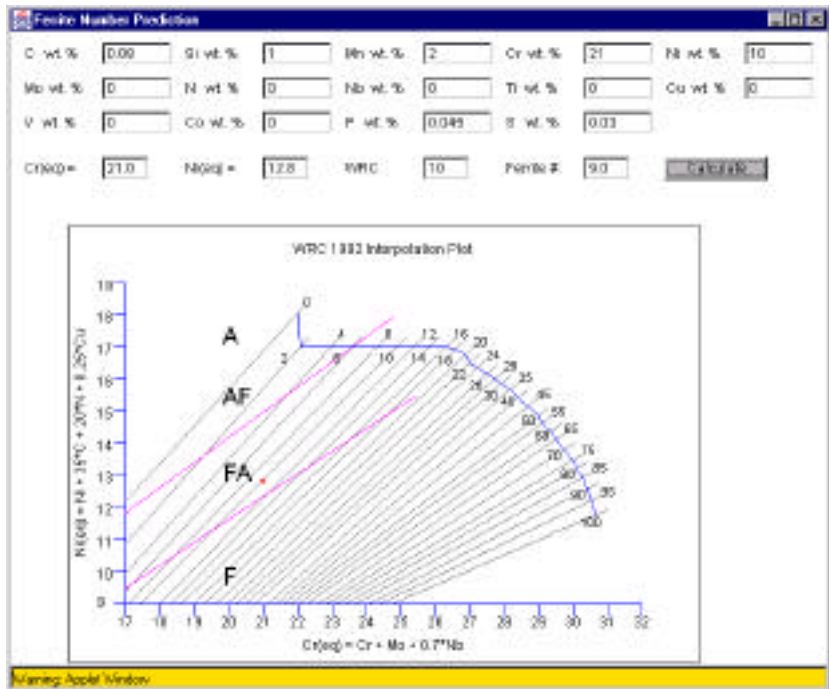
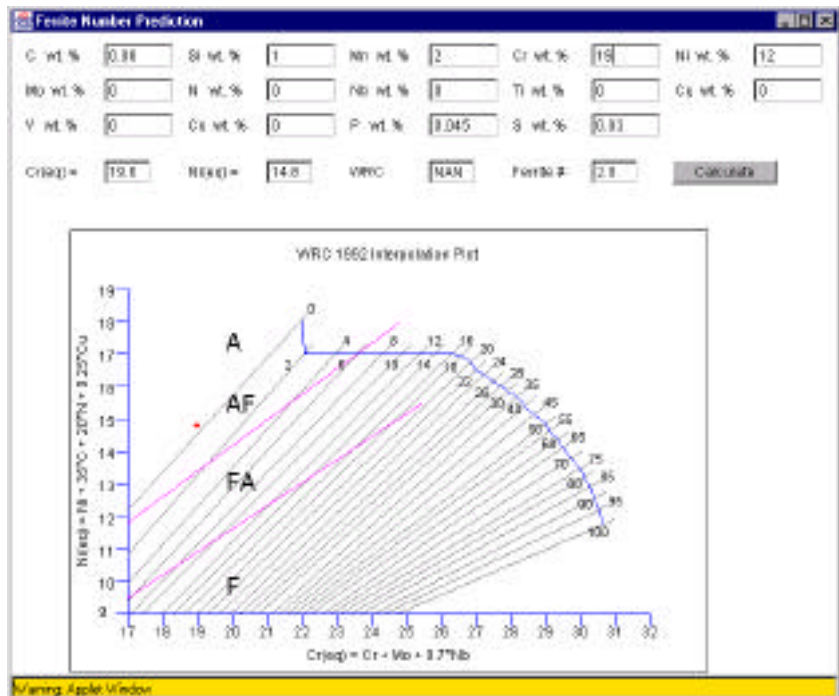


Figure 11b.

Using Cr = 19 %, and Ni = 12%.

This shows the other extreme,  
WRC = Not-A-Number and  
Ferrite # = 2 from the 308 metal  
compositions.



## Tables

Location	Al wt. %
1	4.08
2	4.57
3	4.06
4	3.90
5	4.10
6	3.76
Average	4.08

Table 1. Shows the composition of aluminum wt. % from the scanning electron microscope.

Measurements of Ferrite Number with Feritscope							
Metal	1 <sup>st</sup>	2 <sup>nd</sup>	3 <sup>rd</sup>	4 <sup>th</sup>	5 <sup>th</sup>	6 <sup>th</sup>	Average
W484	12.8	11.4	12.4	12.7	12.8	12.5	12.4
LT-C	14.5	13.4	14.0	12.6	12.5	14.1	13.5

Table 2. Shows the results of the Feritscope on the two weld metals and the average ferrite.

Composition of the weld metal Type 308 (in wt. %)						
C	Mn	Si	Cr	Ni	P	S
0.08	2.0	1.0	19-21	10-12	0.045	0.03

Table 3. Shows the composition of the 308 metal.

Range	Compositions							Ferrite Number	
	C	Mn	Si	Cr	Ni	P	S	WRC	FN(Model)
1	0.08	2.0	1.0	21	10	0.045	0.03	10	9
2	0.08	2.0	1.0	19	12	0.045	0.03	Nan	2

Table 4. Shows the two extremes for the ferrite number.

Figures 9a and 9b show the outputs from the ferrite number model as it appears to the user.